Design and Simulation of a 10 MW Photovoltaic Power Plant using MATLAB and Simulink

Dinut-Lucian Popa[1], Marian-Stefan Nicolae[2], Petre-Marian Nicolae[1], Marius Popescu[1]
[1]Electrical Eng., Energetics and Aeronautics Dept., University of Craiova, Romania
[2]Computer Science Dept., University of Craiova, Romania
pnicolae@elth.ucv.ro

***Abstract*-The paper deals with the components design and the simulation of a photovoltaic power generation system using MATLAB and Simulink software. The power plant is composed of photovoltaic panels connected in series and parallel strings, a DC-DC boost converter and a three-phase inverter which connects to a 0.4 kV three-phase low voltage grid and a 20 kV medium voltage grid by means of a step-up transformer. The DC-DC boost converter uses a MPPT controller and the inverter uses a control method based on d-q theory with a PI current regulator. Some cases for which the dynamic behavior of the configured photovoltaic system presents interest are simulated. They address the solar irradiance and temperature change.**

I. INTRODUCTION

The production of electrical energy without polluting actions and on the environment and depletion of its resources is a very topical problem.

The solar energy radiation, considered relative to the life on Earth, seems to be inexhaustible.

The photovoltaic solar energy relies on the direct generation of electricity by means of silicon cells. Under favorable climate conditions, when shining, the sun provides a power of 1 kW/m^2. The photovoltaic panels allow for direct conversion in electricity of 10…15% from the above mentioned energy [1]. The efficiency of PV system is a permanent concern [2].

The irradiance energy of the sun to electrical energy can be converted through photovoltaic (PV) power generation systems.

If the power generation system does not include batteries to store the DC energy, instead including a common capacitor between the DC-DC and DC-AC converters to store the energy on the side of DC-Link, then a fully non-polluting source is obtained [3].

To get an optimization of the power supplied to the network, depending on the irradiance intensity of the sun, it is preferred to select a configuration in which the photo-voltaic power generation system uses an efficient controller such as Maximum Power Point Tracking (MPPT) [4]-[11].

II. DESIGN OF THE PV POWER GENERATION SYSTEM

The design of a PV power generation system, with an installed power of 10 MW, is proposed in what follows.

The electric power supplying by using a PV equipment is made according to the requirements imposed by the electric energy provider who operates at the PV site, two options being available: the low voltage connection (400 V) and the medium voltage connection (20 kV), by means of the step-up transformer (LV/MV).

The designed PV power generation system is composed of (Fig. 1):

1) A PV array of PV panels grouped in series and/or parallel strings such as to obtain a maximum power of 10 MW;

2) A DC-DC boost converter used as a load regulator and respectively to convert the output voltage of the PV array to a suitable voltage for the inverter;

3) A three-phase DC-AC converter (i.e. inverter) to export the electrical energy to the three-phase grid;

4) A three-phase step-up transformer to adapt the 0.4 kV low voltage output of the inverter to the 20 kV voltage of the grid;

5) The PV power generation system controller, which contains the MPPT controller for the DC-DC boost converter and the inverter's controller.

The MPPT controller is used to control the duty cycle in order to maintain the operating point as close as possible to the maximum power point P_{MP} of the PV array. P_{MP} is located at the intersection between the voltage-current characteristic curve of the PV array and the equivalent load characteristic (Fig. 2).

In Fig. 2, V_{OL} is the open-load voltage of the PV cell, I_{SC} represents its short-circuit current value. I_{MP} and V_{MP} are the current and voltage corresponding to the maximum power point P_{MP}.

An algorithm was conceived and transposed in MATLAB, starting from the initial design data.

A. Design of the PV array

Every panel (module) used by the designed installation consists in cells of series connected polycrystalline cells. The front side of the PV module includes a highly transparent glass sheet, characterized by a significant resistance against mechanic shocks.

The frame of anodized aluminum (covered through electrolysis by a layer of protective oxide), forms the structural support of the module. All these provide an adequate protection against atmospheric agents like hail, snow, ice and storm. Each module contains by-pass diodes introduced in the connection (distribution) box. These diodes will allow the "off-lining" of the modules where the sunshine does not reach, in order to prevent their behavior as consumers for the panels getting radiation from sun and therefore avoiding their undesired heating [12].

978-1-5090-1798-0/16/$31.00 ©2016 IEEE

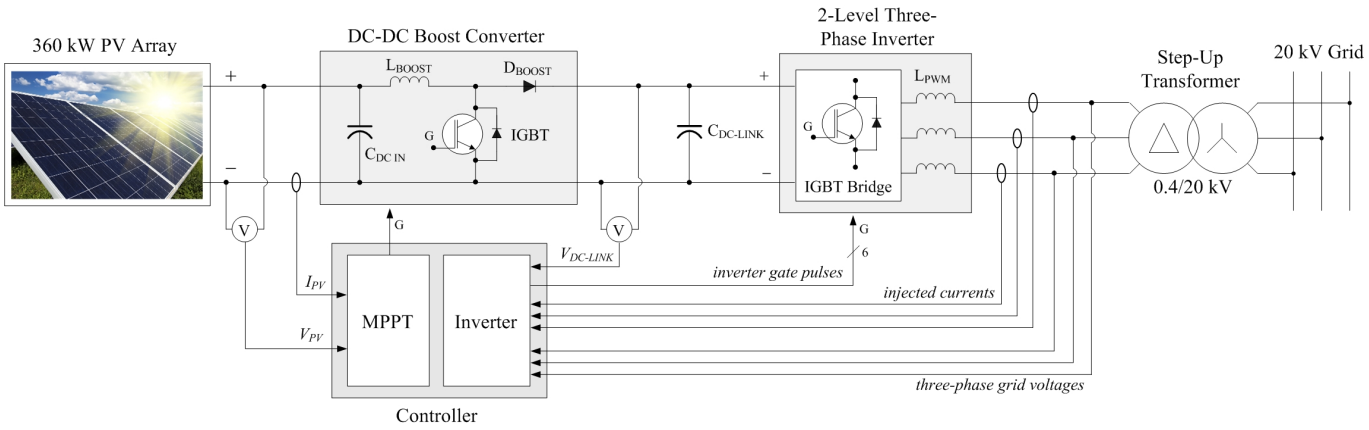

Fig. 1. The basic schematic of one 360 kW photovoltaic array generator.

Several models pf PV cells are available from manufacturers like Mitsubishi, Sharp, Sanyo, LDK, BP Solar, Suntech.

We selected Sanyo HIP-225HDE1 PV modules, with a maximum power of 225 W. The technical specifications for one module are given in Table I.

The number of necessary series-connected modules per string and parallel strings is determined by the DC-DC boost converter input voltage value and the inverter power.

The rated DC input voltage for the boost converter is normally chosen half the output voltage, i.e. the DC-Link voltage.

Considering that the output voltage of a string of series-connected PV modules is the sum of the component modules, and also considering the minimum DC-Link voltage for the inverter, one can obtain the number of PV modules connected in series N_{SER} based on:

$$N_{SER} = \frac{1}{2} \cdot \frac{V_{DC-LINK}}{V_{MP}} \quad (1)$$

with: N_{SER} = number of necessary series connected modules;
$V_{DC-LINK}$ = the DC-Link voltage at the inverter input;
V_{MP} = PV module voltage at maximum power point;

TABLE I
TECHNICAL SPECIFICATIONS OF ONE SANYO HIP-225HDE1 PV MODULE

Cell type	Silicon Polycrystalline
Number of cells per module:	60
Open circuit voltage V_{OC}	41.79 V
Current at maximum power point I_{MP}	6.63 A
Short-circuit current I_{SC}	7.13 A
Voltage at maximum power point V_{MP}	33.9 V
Temperature coefficient of V_{OC}	-0.105 V/°C
Temperature coefficient of I_{SC}	0.00214 A/°C
Temperature coefficient of V_{MP}	-0.101 V/°C
Temperature coefficient of I_{MP}	-0.0006634 A/°C

A lower voltage can be selected for the inverter input, but as the voltage decreases (keeping the output voltage constant), a higher current will flow through the DC-DC boost converter. Therefore higher rated IGBT-s are needed.

The minimum DC-Link voltage for the inverter can be computed with [13]:

$$V_{DC-LINK} \geq 2\sqrt{2} \cdot V_{PHASE} \quad (2)$$

with: V_{PHASE} = the RMS value of the phase voltage at the inverter's output.

Hence, the DC-Link voltage must be greater than 653 V.

Considering (1) and (2), a DC-DC converter input voltage V_{PV} of 350 V and a DC-Link voltage $V_{DC-LINK}$ of 700 V are selected.

Returning to (1), the necessary number of PV modules connected in series N_{SER} shall be rounded to 11. One can now compute the maximum power of a series connected PV string:

$$P_{STRING} = N_{SER} \cdot P_{MP} = 11 \cdot 224.89 = 2.47 \text{ kW} \quad (3)$$

where: P_{MP} = maximum power point.

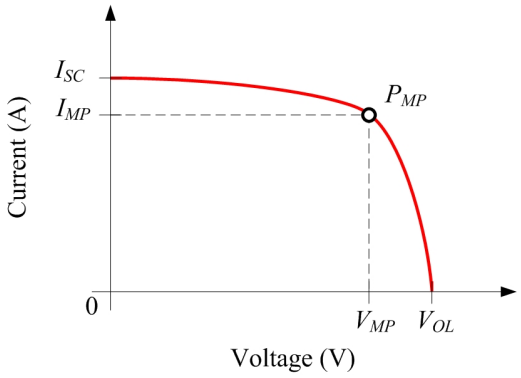

Fig. 2. The Voltage-Current characteristic of a PV cell.

Once the number of series connected modules is set, the number of strings in parallel is computed based on the rated power of one inverter. One selected a 360 kW 2-level inverter offered by IGBT manufacturer Semikron. The necessary number of strings in parallel becomes:

$$N_{PAR} = \frac{P_{INV}}{P_{STRING}} = \frac{360\text{ kW}}{2.47\text{ kW}} = 146 \quad (4)$$

with: P_{INV} = the power of one inverter.

Thus, in order to obtain an installed power of 10 MW, we need a number of inverters N_{INV} and PV arrays N_{ARRAYS} given by:

$$N_{INV} = N_{ARRAYS} = \frac{P_{TOT\ MAX}}{P_{INV}} = \frac{10\text{ MW}}{360\text{ kW}} = 28 \quad (5)$$

with: $P_{TOT\ MAX}$ = desired installed power for the PV park.

The design of the DC-DC-AC converter is done backwards: firstly the inverter and then the DC-DC boost converter.

B. Sizing the DC-AC inverter

Inverter's sizing is done considering the 360 kW PV array's peak output power for a 2-level inverter offered by IGBT manufacturer Semikron. The specialized Semisel online application is used, having the RMS output voltage, output power, efficiency, switching frequency and overload factor as inputs.

For the maximum power of 360 kW and a worst-case efficiency of 85%, the RMS current through inverter is equal to 611.3 A:

$$I_{INV\_RMS} = \frac{P_{INV}}{3 \cdot V_{PHASE}} \cdot \frac{100}{85} = 611.3\text{ A} \quad (6)$$

Sizing the PWM coils inductance is done considering a 5% ripple current from the peak value of the injected current, which is:

$$I_{INV\_PEAK} = I_{INV\_\mathrm{RMS}} \cdot \sqrt{2} = 864.5\text{ A} \quad (7)$$

Hence, the peak-to-peak value of current ripple is:

$$I_{RIPPLE\_PEAK} = 0.05 \cdot I_{INV\_PEAK} = 43.2\text{ A} \quad (8)$$

The PWM coils inductance is calculated with [13]:

$$L_{PWM} = \left(\sqrt{3} \cdot V_{DC}\right) / \left(12 \cdot \delta \cdot f_{COM} \cdot I_{RIPPLE\_PEAK}\right) = 0.62\text{ mH} \quad (9)$$

with: δ = the overload factor;
f_{COM} = the switching frequency of the inverter.

The overload factor δ generated by transients varies within the range [120...180]% [5]. One selected a value of 150% for δ and a switching frequency of 2.5 kHz, considering a compromise between the high cost and bulkiness of the PWM coils for a low switching frequency and the higher losses at a high switching frequency. Also, a higher switching frequency offers a lower THD for the injected current and PCC voltage.

The value of the DC-link capacitor is computed to limit the DC-link voltage ripple to 5% of the DC-Link voltage.

For a sinusoidal waveform, the average value of the current I_{AVG} is 63.6% from the peak value or 0.9 from the RMS value:

$$I_{AVG} = 0.9 \cdot I_{INV\_RMS} = 0.9 \cdot 611 = 550.18\text{ A} \quad (10)$$

The peak-to-peak ripple value of the DC-Link voltage is imposed to 5%:

$$V_{RIPPLE\_PEAK} = 0.05 \cdot V_{DC-LINK} = 0.05 \cdot 700 = 35\text{ V} \quad (11)$$

The capacitor's value $C_{DC\text{-}LINK}$ can now be determined with [13]:

$$C_{DC-LINK} \geq \frac{I_{INV\_AVG}}{2 \cdot \omega \cdot V_{RIPPLE\_PEAK}} \geq \frac{550{,}18}{2 \cdot 314 \cdot 35} \geq 25018\ \mu\text{F} \quad (12)$$

where: ω = the angular frequency corresponding to the 50 Hz grid.

The rated voltage V_{RATED_CDC} is recommended to be at least 20 % higher than the operating voltage:

$$V_{RATED\_CDC} \geq 120\% \cdot V_{DC-LINK} \geq 840\text{ V} \quad (13)$$

Considering (12) and (13), several capacitors must be connected in parallel to achieve the large capacitance needed at this high voltage value.

The chosen IGBT switching transistors of the inverter are SKiiP3614GB12E46DUW, liquid cooled.

C. Sizing the DC-DC boost converter

The parameters imposed for the DC-DC boost converter are centralized in Table II.

Considering these values, the chosen IGBT switching transistor and diode of the boost converter is one SKiiP3614GB12E46DUW module, liquid cooled.

TABLE II
TECHNICAL SPECIFICATIONS OF THE DC-DC BOOST CONVERTER

Rated input voltage	350 V
Minimum input voltage V_{MIN}	300 V
Rated output voltage $V_{DC\text{-}LINK}$	700 V
Rated output voltage I_{OUT_RMS}	611 A
Switching frequency f_{COM_BOOST}	2 kHz

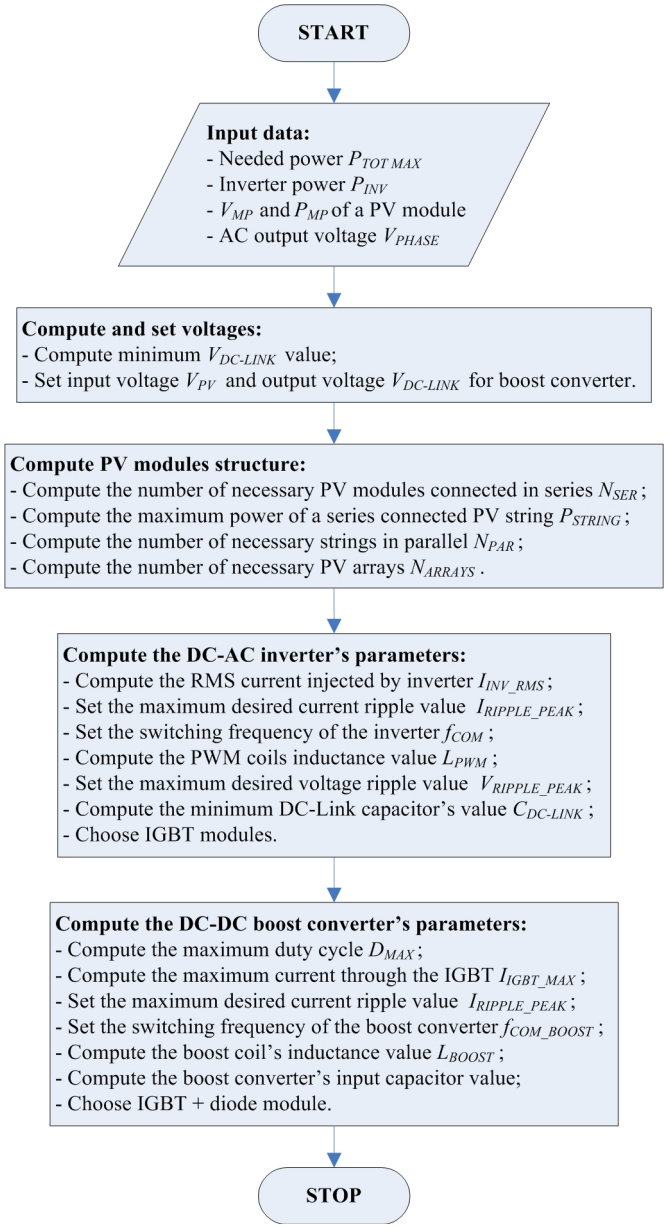

Fig. 3. The flowchart of the photovoltaic system design.

The specialized Semisel online application was used.

Considering the boost converter's coil resistance of 35 mΩ and the IGBT and diode losses, the efficiency η of the converter is estimated to be 90%.

The duty cycle D_{MAX} at the minimum input voltage V_{MIN} can be computed with [14]:

$$D_{MAX} = 1 - \frac{V_{MIN} \cdot \eta}{V_{DC-LINK}} = 0.61 \quad (14)$$

The maximum current through the IGBT can be computed with [14]:

$$I_{IGBT\_MAX} = 2 \cdot I_{OUT\_RMS} \cdot \left(D_{MAX} + 1\right) = 1973.6 \text{ A} \quad (15)$$

Sizing the L_{BOOST} coil inductance is done considering a 5% ripple current from the maximum current through the IGBT. Hence, the peak-to-peak value of current ripple is:

$$I_{RIPPLE\_PEAK} = 0.05 \cdot I_{IGBT\_MAX} = 98.6 \text{ A} \quad (16)$$

The minimum L_{BOOST} coil inductance is calculated with [14]:

$$L_{BOOST} \geq \frac{V_{MIN} \cdot \left(V_{DC-LINK} - V_{MIN}\right)}{I_{RIPPLE\_PEAK} \cdot f_{COM\_BOOST} \cdot V_{DC-LINK}} \quad (17)$$

Considering (17), the minimum inductance is computed as 0.89 mH, so a 1 mH boost inductor is chosen.

An input capacitor in necessary for the boost converter's stability. Considering the power involved, a 100 μF input capacitor is selected [16].

The flowchart of the photovoltaic system design is depicted in Fig. 3.

III. Simulation of One 360 kW Photovoltaic Array Generator

By using the designing parameters of the PV park presented below and the data from datasheet, a simulation of a field with PV cells corresponding to one of the 28 inverters was done in the Simulink module which belongs to MATLAB.

The Simulink model of the PV field is built by using elements from the library SimPowerSystems. The solving method is of discrete type and uses a fix step of 1 μs. The control system operates at a sampling step of 100 μs, in order to reproduce as accurate as possible the digital control and respectively to be appropriate for loading in microcontrollers and in developing platforms as dSPACE is.

The Simulink model of the generating PV system includes:

- an instrument to build signals related to solar radiation and panels temperature (Signal Builder Tool), in order to test the generation system's reactions in different contexts;
- the field with PV cells;
- the DC-DC converter, along with the dedicated control system MMPT (Maximum Power Point Tracking);
- the three-phase inverter along with the dedicated control system;
- the step-up transformer for connection to the network, of 0.4/20 kV;
- the network of 20 kV toward which the generated electric power is transferred.

The model of PV field includes the configuration of the number of PV cells in series and in parallel, as well as the possibility to access different predefined models of panels from several manufacturers. The module Sanyo HIP-225HDE1 was selected.

The control system MPPT allows for a maximal energy recovering, irrespective to temperature and illumination. The voltage V_{PV} and the current I_{PV} are continuously measured in

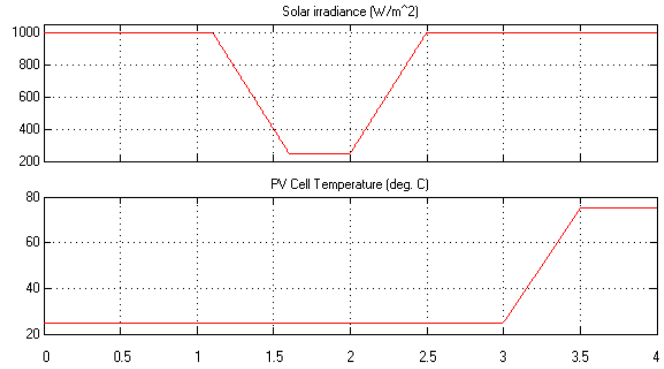

Fig. 4. The evolution of the solar irradiance (top) and PV cell temperature (bottom) during simulation.

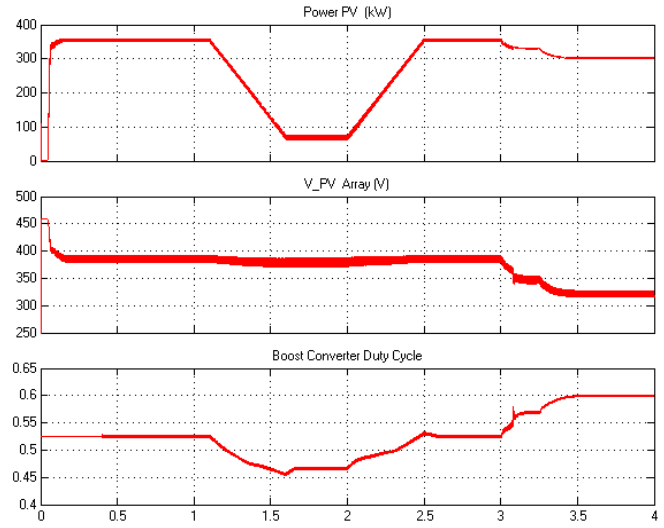

Fig. 5. The waveforms at the boost converter side during simulation: the output power (top), the input voltage (middle) and the duty cycle (bottom).

order to deduce the power extracted from the panel. The power is compared to its previous value. After comparison, the voltage at panel's terminals is increased or reduced by means of the duty cycle from the input of the PWM generator.

The control of the three-phase inverter is performed such as to export the power provided by the PV field in the AC network of 0.4 kV, respectively of 20 kV and to preserve a constant voltage of 400 V at the output terminals, along with a constant voltage of 700 V across the DC bars, irrespective to the operating conditions (power of PV panels). It consists of a block for test and transformation into the *d-q* coordinates, a DC voltage regulator, a current regulator, a reference voltage generator and a PWM generator for 2-Level three-phase inverters.

The model of the network in which the PV generating system exports power includes a MV load, step-up transformers, models for long lines and an equivalent generator of 24 kV connected by using a step-up transformer 24/120 kV.

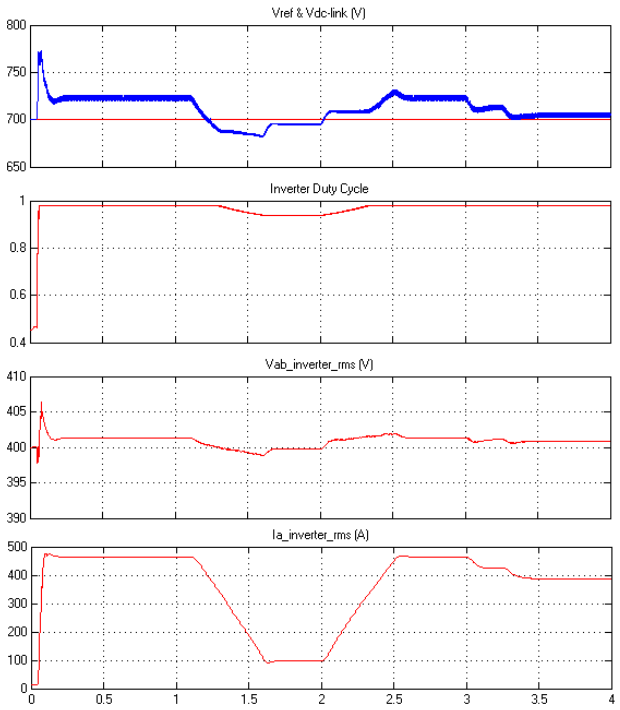

Fig. 6. The waveforms at the inverter side during simulation. From top to bottom: the reference and measured DC-Link voltage, the duty cycle, the RMS line voltage, the RMS phase current.

The inverter's control pulses are inputs for a block used to introduce switching outages of 3 μs, in order to avoid the short-circuits between the IGBT-s from the same side.

The chain of events was selected to last 4 seconds, as follows (Fig. 4):

- the solar radiation has an initial value of 1000 W/m^2, (regular value), than falls up to 250 W/m^2 , smoothly along 0.5 seconds in order to simulate the apparition of some clouds;
- in the 2nd second, the solar radiation comes back to 1000 W/m^2 along a period of 0.5 seconds;
- the temperature of the PV cells is increased from 25°C up to 75°C beginning with the 3rd second, along 0.5 sec.

The evolution of voltage and power of the PV field is depicted by Fig. 5. The panels' power decreases from 360 kW (corresponding to maximum solar radiation) up to 80 kW at 250 W/m^2. One can notice that the voltage does not decrease significantly. It means that the control algorithm MPPT operates in a correct manner by limiting the current injected into the network. Close to the end of the simulation period, the input voltage decreases up to 320 V because the PV cells increases. The duty cycle increases to 0.6 to keep the output voltage constant (Fig. 5).

The waveforms at the inverter side during simulation are depicted by Fig. 6. No large deviations from the DC-Link reference voltage or the RMS standard 400 V voltage value on the LV bus are observed.

The active powers in the conversion chain are depicted by Fig. 7. The efficiency of the power conversion depends

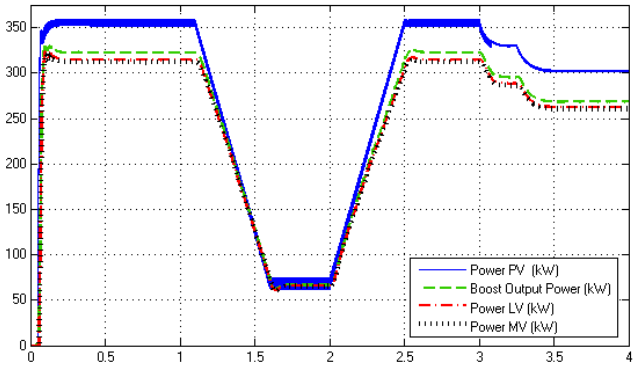

Fig. 7. The evolution of the active powers during simulation, from the PV array to the MV grid.

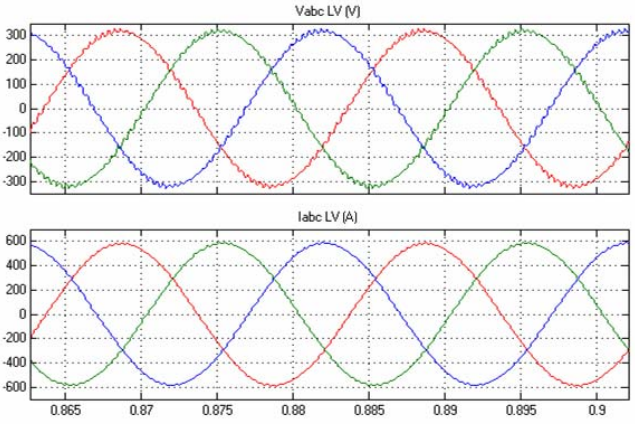

Fig. 8. Detail of the waveforms of the phase voltages (top) and currents (bottom) at the output of the inverter.

greatly on the boost and coupling inductors resistances. An efficiency of 0.88 is obtained for the boost converter and an efficiency of 0.94 is obtained for the inverter.

In order to estimate the harmonic distortion level for the voltage in the 0.4 kV bars, as well as the current injected into the network, a special analysis tool was used (FFT Analysis Tool) from the user graphic interface "PowerGUI". By using this instrument one can notice the efficiency of the coil used for coupling to the network with the switching frequency 2.5 kHz and small values for the harmonic distortion of voltage (2.3%) and respectively for current (0.8%). The waveforms of the phase voltages and currents at the output of the inverter are depicted in Fig. 8. In the 20 kV the total harmonic distortion is even smaller (< 1%) because of the transformer's inductance.

IV. CONCLUSIONS

The simulation of the designed PV park by using Simulink made possible the testing and observation of its stability and efficiency. The PV generation system behaves well in different conditions of solar radiance and temperature of PV panels, preserving its stability and succeeding in extracting the maximum power from the PV panels owing to the control algorithm MPPT.

The PV generation system is also providing a voltage characterized by a very good quality: the total harmonic distortion in the 0.4 kV panels has a low value (2.3%) and in the 20 kV bars the distortion is even smaller (< 1%).

These conclusions can be deduced based on the obtained data and waveforms. We can conclude that the PV generating system was designed properly.

REFERENCES

[1] J. M. Carrasco, L. G. Franquelo, J. T. Bialasiewicz, E. Galvan, R. C. P. Guisado, Ma. A. M. Prats, J. I. Leon, N. Moreno-Alfonso, "Power-Electronic Systems for the Grid Integration of Renewable Energy Sources: A Survey", *IEEE Trans. on Ind. Electr.*, Vol. 53, Issue 4, June 2006, pp. 1002 – 1016.

[2] M, A. Green, K. Emery, Y. Hishikawa and W. Warta , „Solar cell efficiency tables (version 37)." *Progress in Photovoltaics: Research and Applications*, vol. 19, pp. 84-92 (2011).

[3] B. J. Szymanski, K. Kompa, L. Roslaniec, A. Dmowski and J. Szymanski, "Operation of photovoltaic power systems with energy storage", *2011 7th International Conference-Workshop on Compatibility and Power Electronics (CPE)*, Tallinn, 2011, pp. 86-91.

[4] N. O. Cherchali, A. Morsli, M. S. Boucherit, L. Barazane and A. Tlemçani, "Comparison of two maximum power point trackers for photovoltaic systems using robust controllers," *2014 3rd International Symposium on Environmental Friendly Energies and Applications (EFEA)*, St. Ouen, 2014, pp. 1-5.

[5] R.-L. Lin, C. Hong-Zhi, "MPPT photovoltaic wide load-range ZVS phase-shift full-bridge charger with DC-link current regulation", *2012 IEEE Industry Applications Society Annual Meeting* (IAS), pp.1-8, 7-11 Oct. 2012.

[6] M. A. G. de Brito, L. P. Sampaio, G. Luigi, G. A. e Melo and C. A. Canesin, "Comparative analysis of MPPT techniques for PV applications", *2011 Int. Conf. on Clean Electrical Power (ICCEP)*, Ischia, pp. 99-104, 2011.

[7] H. Guan-Chyun, C. Hung-Liang, C. Yaohwa, T. Chee-Ming, S. Shian-Shing, "Variable frequency controlled incremental conductance derived MPPT photovoltaic stand-along DC bus system", *Twenty-Third Annual IEEE Applied Power Electronics Conference and Exposition (APEC)*, pp.1849-1854, 24-28 Feb. 2008.

[8] H. Guan-Chyun, C. Hung-Liang, T. Cheng-Yuan, W. Chi-Hao, "Photovoltaic Power-Increment-Aided Incremental-Conductance MPPT With Two-Phased Tracking", *IEEE Transactions on Power Electronics*, vol.28, no.6, pp.2895-2911, June 2013.

[9] Li Sheng-qing; Zhang Bin; Xu Tian-jun; Yang Jun, "A new MPPT control method of photovoltaic grid-connected inverter system", *The 26th Chinese Control and Decision Conference (2014 CCDC)*, pp. 2753-2757, 2014.

[10] W. Hongbin, T. Xiaofeng, "Three phase photovoltaic grid-connected generation technology with MPPT function and voltage control", *Int. Conf. on Power Electr. and Drive Systems (PEDS 2009),* pp. 1295-1300, 2-5 Nov. 2009.

[11] M.I. Hossain, S.A. Khan, M. Shafiullah, M.J. Hossain, "Design and implementation of MPPT controlled grid connected photovoltaic system", *2011 IEEE Symposium on Computers & Informatics (ISCI)*, pp. 284-289, 20-23 March 2011.

[12] J. Simon and G. Mosey, "Feasibility Study of Economics and Performance of Solar Photovoltaics at the Sky Park Landfill Site in Eau Claire, Wisconsin", *National Renewable Energy Laboratory*, available at http://www.nrel.gov/docs/fy13osti/56995.pdf (2013).

[13] G. K. Kasal and B. Singh, "Voltage and Frequency Controllers for an Asynchronous Generator-Based Isolated Wind Energy Conversion System", *IEEE Trans. on Energy Conv.*, Vol. 26, Issue 2, pp. 402-416, 2011.

[14] Brigitte Hauke, "Basic Calculation of a Boost Converter's Power Stage", *Texas Instruments Application Report SLVA372C,* 2014.

[15] Robert W. Erickson, *DC–DC Power Converters*, Wiley Encyclopedia of Electrical and Electronics Engineering, 2007.

[16] J. Arai, T. Takada, K. Koyanagi and R. Yokoyama, "Power Smoothing by Controlling Stored Energy in Capacitor of Photovoltaic Power System", *Power and Energy Engineering Conference (APPEEC)*, 2012 Asia-Pacific, Shanghai, 2012, pp. 1-5.